

Insulation Integrity in GIS under Particle Contamination

G V Nagesh Kumar, Associate professor, JNTUA College of engineering, Pulivendula
 D.DeepakChowdary-Dr L Bullaya College of Engineering karanam2010@gmail.com
 K.Appala Naidu-Assistant professor in Vignan institute of information and technology
 K.NAVYA- M.Tech student in Vignan institute of information and technology

Abstract: SF6 gas filled in the bus ducts of Gas Insulated substations (GIS) are very sensitive to field disturbance. These disturbances are caused by conductor surface imperfections and by particle contaminations (spherical, cylindrical) due to improper manufacturing. Due to these contaminations, operation of GIS under high fields is also affected. Hence, if the effects of these contaminations can be reduced then the reliability of GIS can be improved to a great extent and operation of GIS at high fields can be possible. In this paper, analysis on movement of particle inside gas insulated bus duct (GIB) with different dimensions and positions has been done so as to examine the reduction in insulation strength due to particle contamination. Metal inserts (MI) have been used to reduce electric field stress and to increase insulation strength. The results obtained have been presented for future reference.

Keywords: SF6 gas, GIS, Particle contaminations, Insulation strength, Electric field stress, MI.

1. Introduction:

Population increase demands high energy. Non – renewable energy resources are been replaced by renewable energy sources to maximum meet the energy demands. In this context, it is often required to improve the reliability of transmission and distribution system by ensuring that the innovations do not affect the environment. GIS has found great importance in meeting the growing electricity demands. SF6 gas manufactured is mostly used in GIS and circuit breakers. Due to few improper manufacturing reasons, some disturbances such as voids, delamination, protrusion, spherical and cylindrical type particle contaminations which are conductive are found which greatly affect the insulation strength of SF6 gas and electric field stress in GIS. These particles can also reduce power frequency lighting and switching voltage strength of the insulation of the GIS.

Many investigations were carried in order to reduce the effects of particle contamination. To reduce the particle effect, particle movement and trapping of electro static particle was introduced but were not so effective in reducing the electric field stress. Hence, Functionally graded materials were used to improve the breakdown strength of the voltage of solid insulator by keeping simple structure. Solid insulator called as spacers plays an important role in GIS. In case of any defects on these spacers, there will be an increase in electric field stress along the surface of the spacers and at the triple junction. This may not allow the use of GIS in high voltage applications.

Particle Contamination of solid insulator surfaces can result in surface flash over well below the clean breakdown voltage for insulators. Spacers design and shape plays a vital role in improving the insulation strength and reducing the electric field stress. Among a number of spacer designs, post type, disc type and cone type are few designs commonly used. In this paper we are analyzing using cone type spacer. Metal inserts also play an important role in controlling the electric field stress.

In this paper we are trying to reduce the electrical field stress and improve the insulation strength of the SF6 gas by using FGM. In FGM few types like ascending, descending

and u shape etc., material distribution can be done by using centrifugal force method. By the presence of metal inserts inside the SF6 gas, the insulation strength of the gas has been reduced at the triple junction (formed by gas, spacer and conductor) formed by the presence of particle contaminations which are conductive (Al, Cu and Ag. Small particles do not cause large reduction in the break down strength of the voltage. Longer particles may cause reduction in the insulation performance. The position of particle will also affect insulation by increasing the electrical field stress. So, we are computing stress values by keeping particle contaminations at various positions and dimensions (by increasing the length) and the obtained results are presented for reference.

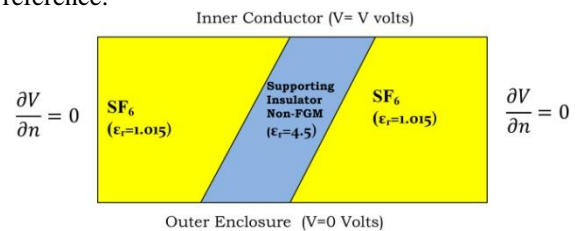


Fig.1 Functionally graded materials for spacers

2. Computation of Electric Field:

SF6 gas has found high importance in GIS due to higher dielectric strength than air and sub-station clearances required are smaller in GIS than in air substations because of high dielectric strength of SF6. In GIS main employed insulating media are SF6 gas and spacers. Hence any defects in them will overall affect the operating condition of GIS. It is mandatory to check the electric field stress to improve the reliability of GIS.

Computation of electric field stress is necessary for improving the reliability of GIS and so many researchers have proposed methods for its computation. Methods like Charge Simulation method, FEM, etc was introduced and among them FEM was considered to be most efficient method especially when it involved in complex modeling problems. The electrostatic field in anisotropic dielectric material under steady state conditions by assuming Cartesian coordinate system and Laplacian field, the electrical energy W stored within the whole volume U of the region is

considered as:

$$W = \frac{1}{2} \int_u \epsilon |\text{grad}V|^2 du \tag{1}$$

$$W = \frac{1}{2} \iiint \left[\epsilon_x \left(\frac{\partial V_x}{\partial x} \right)^2 + \epsilon_y \left(\frac{\partial V_y}{\partial y} \right)^2 + \epsilon_z \left(\frac{\partial V_z}{\partial z} \right)^2 \right] dx dy dz \tag{2}$$

Moreover, when minute level field behaviour is considered, the problem can be treated as two dimensional. The total stored energy within this area-limited system is given as

$$\frac{W}{\phi} = \frac{1}{2} * \epsilon \iint \left[\left(\frac{\partial V_x}{\partial x} \right)^2 + \left(\frac{\partial V_y}{\partial y} \right)^2 \right] dx dy \tag{3}$$

Where (W/φ) is energy density per elementary area dA.

Assumptions considered for applying minimisation criteria on the above equations are

- Potential distribution V(x,y,z) is continuous over the region and
- Its derivative may exist.

Since it is impossible to find a continuous function for the entire area A, an ample discretization must be made. Hence, the area under consideration is further subdivided into triangular elements thus:

$$\frac{W}{\phi} = \frac{1}{2} * \epsilon * \sum_{i=1}^n \left[\left(\frac{\partial V_x}{\partial x} \right)^2 + \left(\frac{\partial V_y}{\partial y} \right)^2 \right] * A_i \tag{4}$$

where n is the total number of elements and A_i is the area of the ith triangle element. Hence, the formulation regarding the minimisation of the energy within the complete system may be written as

$$\frac{\partial X}{\partial [V(x,y)]} = 0; \text{ where } X = \frac{W}{\phi} \tag{5}$$

The result is an approximation for the electrostatic potential for the nodes at which the unknown potentials are to be computed. Within each element the electric field strength is considered to be constant and the electric field strength is calculated as

$$E = -i \frac{\partial V(x,y)}{\partial x} - j \frac{\partial V(x,y)}{\partial y} \tag{7}$$

Fig.(1) represents the numerical model of the problem under study.

3. Particle infusion in GIS:

Dust and contamination particles in SF₆ gas greatly reduce the insulation strength of compressed SF₆ gas. Hence the contamination in the form of conducting particles should be observed and controlled by some means to retain the insulation strength. Even the electrical insulation performance of GIS systems is seriously affected by these contamination particles.

Main causes for the contamination particles were found to be due to conductors mechanical load changes and movement of various modules during transportation and commissioning. Also, it can be noticed that under an applied electric field in a horizontal coaxial GIS system, a conducting particle resting on the enclosure base acquires a charge and will rise against the gravitational force due to the central conductor at sufficiently high. If any particles attaches to the epoxy insulator surface, insulation will be severely weekend.

While machining, the sharp edges and burrs on the conductor surface may gradually reduce the life of GIS modules. Though a complete elimination of particles in GIS cannot be done, an investigation for detecting and localizing their effect is going on. Using Partial discharge detection method, particles can be easily detected but those on spacers are difficult to detect. In this analysis, to improve the insulation strength and to reduce the electric field stress, metal inserts have been utilized.

4. Results and Discussions:

A normal cone type spacer with clearance between outer and inner electrodes of 100mm has been designed in COSMOL software. Inner electrodes were applied with voltages of 72.5, 145 and 220 KV with outer electrode grounded. The bus duct is filled with SF₆ gas and relative permittivity of 1.015 is considered. FGM spacer and three cases of permittivity distribution i.e. GH, GL, and U are considered for analysis. Considering different dimensions and positions of particle contamination, electric field stress is increased and insulation strength is greatly reduced with surface flashovers at the triple junctions. With the use of MI, results in the reduction of electric field stress are shown in the table and graphs.

Figures 1(a) and 1(b) represents electric potential in cone type spacer when without metal insert and with metal insert. Figures 2(a) to 2(x) represents electric field stress without and with metal inserts when considered different positions and dimensions for a GH FGM cone type spacer. From these figures it is clear that without metal inserts electric field stress increases and with the use of metal inserts there is a drastic reduction of electric field stress. The corresponding values for electric field stress at inner and outer electrodes without and with MI for different positions and dimensions for GH FGM spacer have been recorded and tabulated in table 1. From table 1 it is clear that without MI, as the applied voltage increases, electric field stress at the inner and outer electrode ends increases. When MI has been included then the electric field stress at the inner and outer electrode reduces drastically.

Analysis on a GL FGM cone type spacer for different dimensions and positions resulted in figures 3(a) to 3(x). The analysis has been carried for four positions and three dimensions without and with MI. These figures clearly indicate that the use of MI when compared to without MI in the spacer decreases electric field stress at inner and outer electrode ends. This implies that MI offers the advantage of reduction of electric field stress. Correspondingly the tabulated results of table 2 clearly shows that without and with MI, as the voltage increases the electric field stress at inner and outer electrode end increases. Again it is obvious that when metal inserts are introduced the reduction of electric field stress can be clearly seen in the table. The table also gives idea of electric field stress at inner and outer electrodes for different positions and dimensions.

Next a U FGM cone type spacer was designed with and without MI and analysis of electric field stress at inner and outer electrode ends for 3 dimensions and 4 positions were carried and resulted in figures from 4(a) to 4(x). These figures give an idea that the use of MI when compared without MI greatly reduces electric field stress at inner and

outer electrode ends. Also the corresponding tabulated results of table 3 clearly explains that with MI when compared without MI, we can drastically reduce electric field stress at inner and outer electrode ends for different applied voltage. It is also clear that electric field stress at inner and outer electrode end is lowest at the applied voltage of 72.5KV when compared with the voltages of 145 and 220KV. Table also includes values at four different positions corresponding to three dimensions.

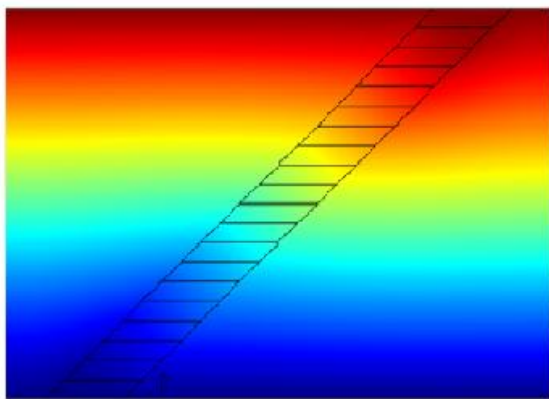
5. Conclusions:

In the present work, simulation of particle trajectory of a single phase GIB has been proposed. The movement patterns of Copper metallic particles at 72.5KV, 145KV, 220KV under power frequency on the particle have been studied by developing a COMSOL software program. From the resultant figures and corresponding tabulated results at three different dimensions and four different positions, the following points can be concluded:

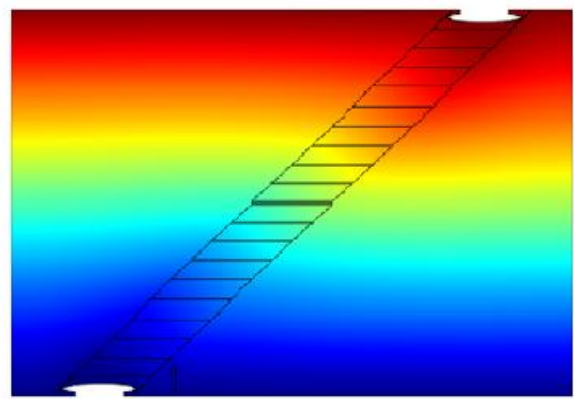
- The lowest value of electric field stress at inner and outer electrode end with and without MI can be noted at the

lowest applied voltage of 72.5KV. At applied voltages of 145 and 220 KV, electric field stress increases at inner and outer electrode ends.

- The particle contamination resulted in the breakdown of insulation strength due to increase of electric field stress. Hence analysis was carried on movement of particle inside GIS at different dimensions and positions to check the reduction of electric field stress so as to maintain the reliability of GIS.
- Analysis has carried at three grading that is GH, GL and U with and without MI and the results were presented.
- Including metal inserts in our design also shows that there can be a drastic reduction of electric field stress at both inner and outer electrode ends when compared without metal inserts. This enables to retain the insulation strength thereby improving the operating condition of GIS.

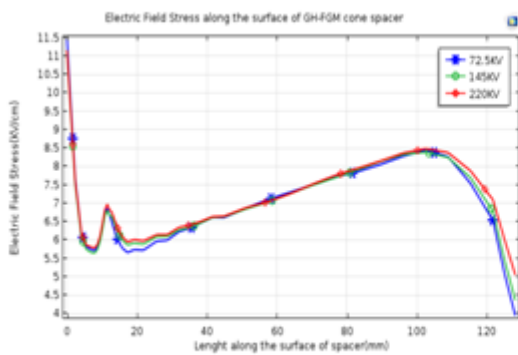


(a) Without MI

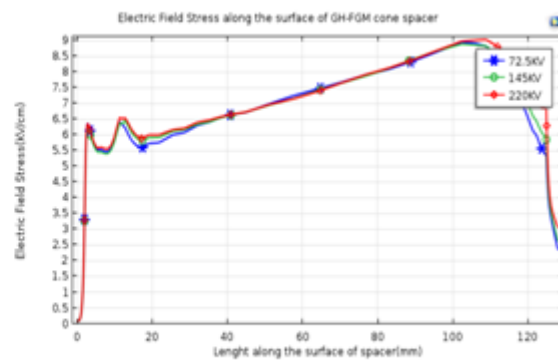


(b) With MI

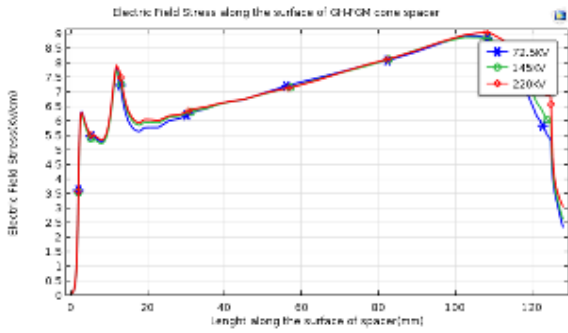
Fig. (1) Electrical Potential



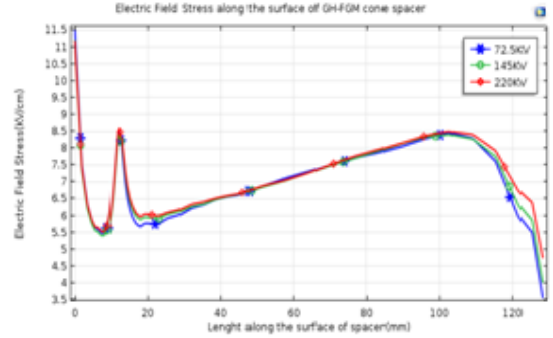
(a) At position 1 and dimension 1 without MI



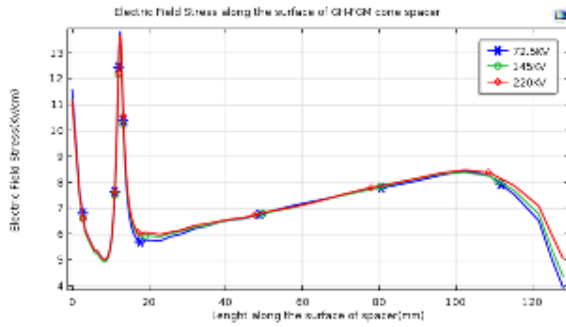
(b) At position 1 and dimension 1 with MI



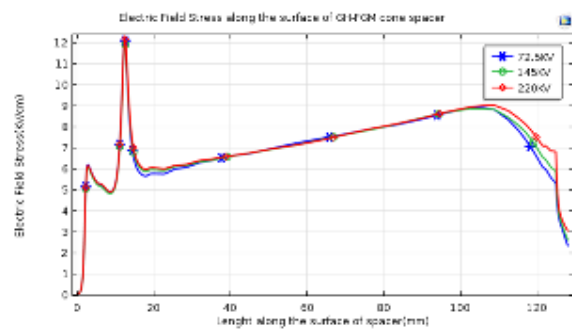
(c) At position 1 and dimension 2 without MI



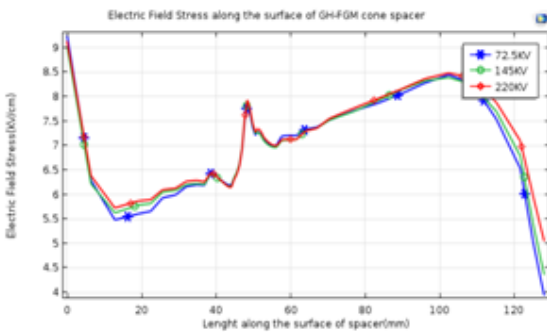
(d) At position 1 and dimension 2 with MI



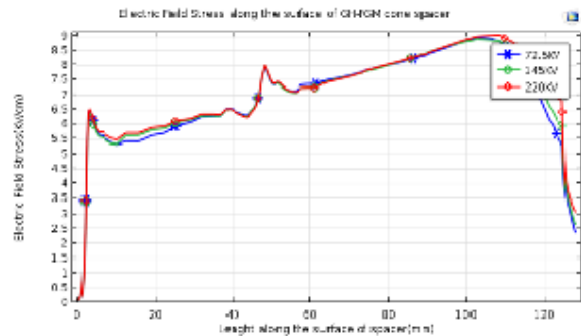
(e) At position 1 and dimension 3 without MI



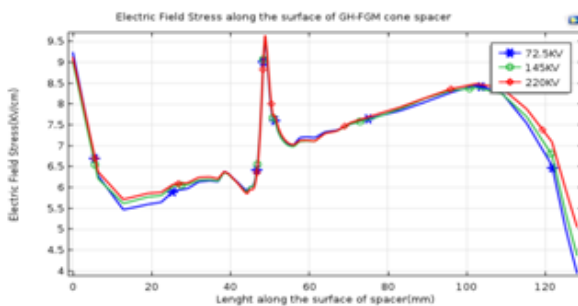
(f) At position 1 and dimension 3 with MI



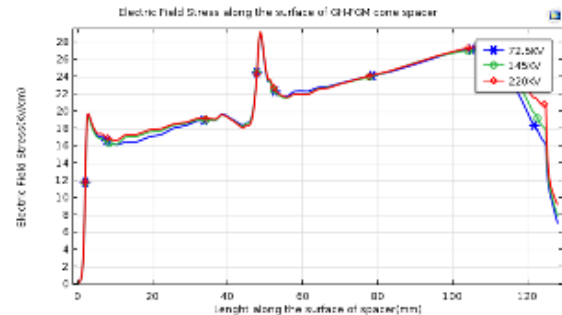
(g) At position 2 and dimension 1 without MI



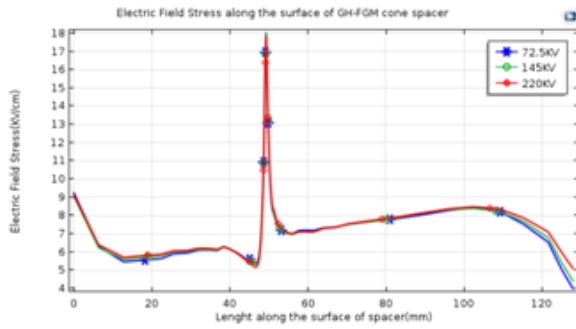
(h) At position 2 and dimension 1 with MI



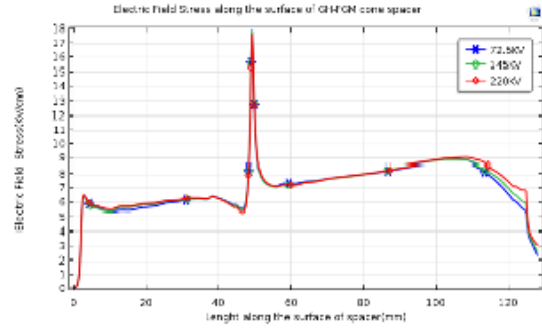
(i) At position 2 and dimension 2 without MI



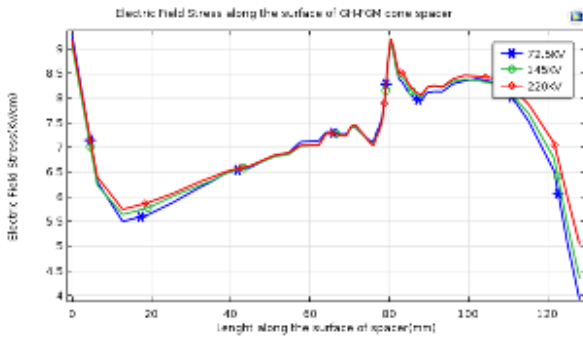
(j) At position 2 and dimension 2 with MI



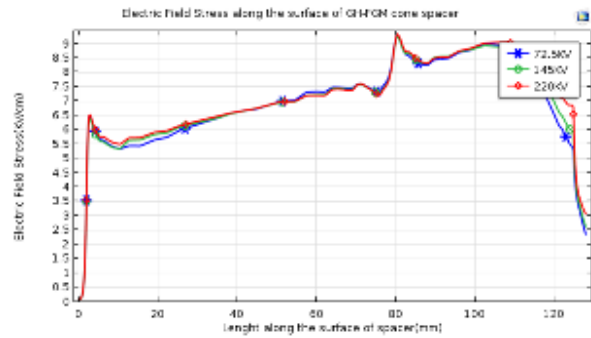
(k) At position 2 and dimension 3 without MI



(l) At position 2 and dimension 3 with MI



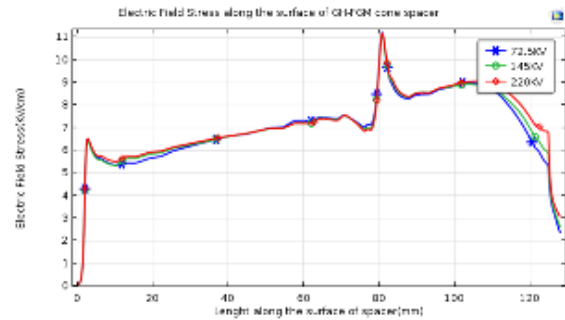
(m) At position 3 and dimension 1 without MI



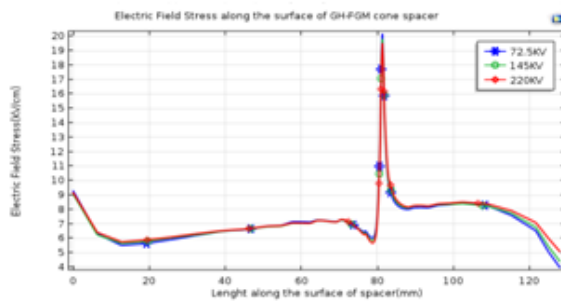
(n) At position 3 and dimension 1 with MI



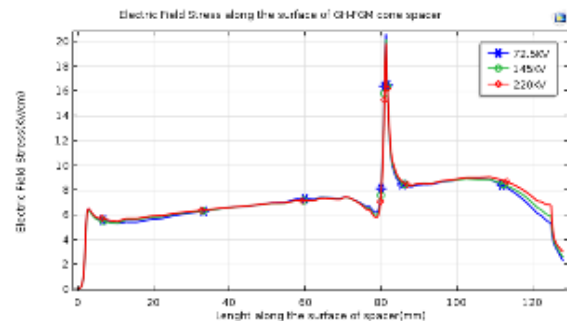
(o) At position 3 and dimension 2 without MI



(p) At position 3 and dimension 2 with MI



(q) At position 3 and dimension 3 without MI



(r) At position 3 and dimension 3 with MI

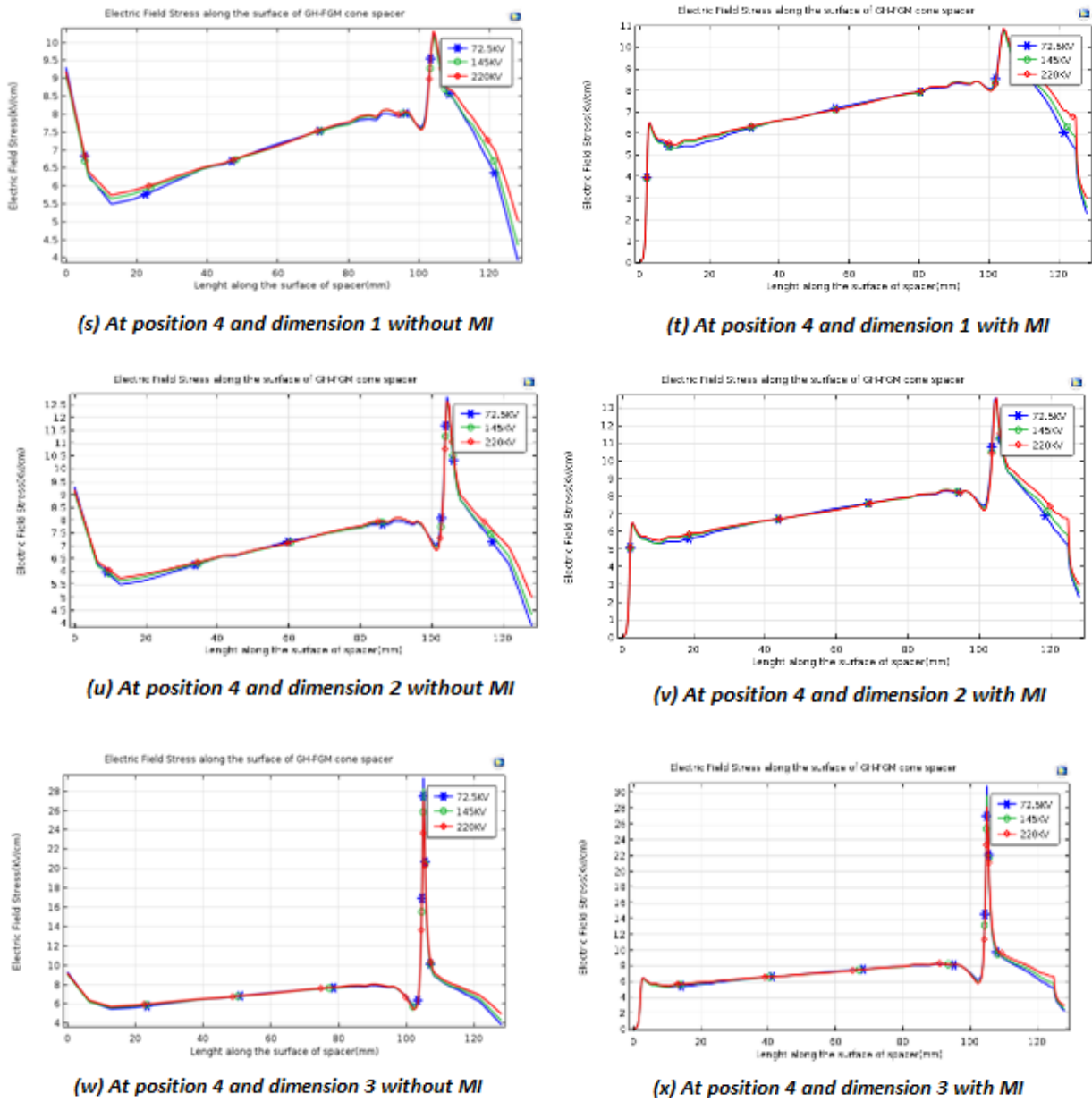
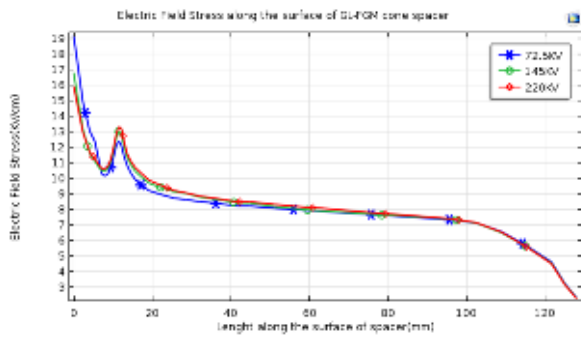


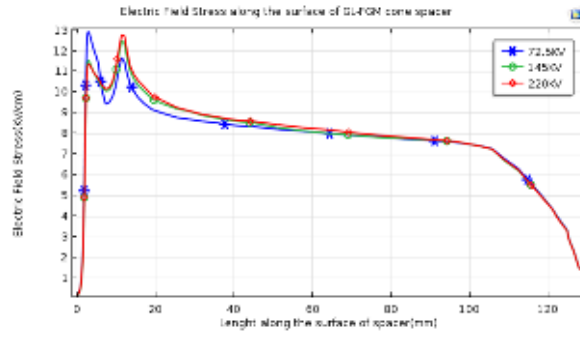
Fig. 2 Electric field stress for a GH FGM spacer for different dimensions and positions

Type	Applied Voltage	72.5KV												145KV												220KV											
		Electric Field Stress Inner Electrode End (KV/CM)						Electric Field Stress outer Electrode End (KV/CM)						Electric Field Stress Inner Electrode End (KV/CM)						Electric Field Stress outer Electrode End (KV/CM)						Electric Field Stress Inner Electrode End (KV/CM)						Electric Field Stress outer Electrode End (KV/CM)					
		wmi			wmi			wmi			wmi			wmi			wmi			wmi			wmi			wmi			wmi			wmi			wmi		
		dim-1	dim-2	dim-3	dim-1	dim-2	dim-3	dim-1	dim-2	dim-3	dim-1	dim-2	dim-3	dim-1	dim-2	dim-3	dim-1	dim-2	dim-3	dim-1	dim-2	dim-3	dim-1	dim-2	dim-3	dim-1	dim-2	dim-3	dim-1	dim-2	dim-3	dim-1	dim-2	dim-3	dim-1	dim-2	dim-3
GH-FGM	positi on-1	11.46	11.54	11.61	0.098	0.097	0.098	3.923	3.355	3.324	2.34	2.307	2.332	22.93	23.07	22.98	0.196	0.195	0.195	7.866	7.111	7.787	4.68	4.634	4.665	34.78	35.01	35.13	0.297	0.296	0.296	11.94	10.79	11.94	7.1	7.061	7.078
		11.15	11.21	11.25	0.097	0.096	0.096	4.361	4.009	4.362	2.609	2.597	2.603	22.31	22.42	22.29	0.194	0.193	0.193	8.722	8.019	8.634	5.218	5.194	5.205	33.65	34.01	34.17	0.294	0.293	0.297	13.23	12.17	13.24	7.916	7.881	7.897
		11.15	11.18	11.1	0.1	0.099	0.099	5.046	4.742	5.048	3.049	3.039	3.044	22.31	22.36	22.17	0.2	0.198	0.196	10.09	9.483	9.990	6.079	6.088	6.088	33.64	33.93	33.99	0.303	0.301	0.3	15.31	14.39	15.32	9.251	9.223	9.238
	positi on-2	9.253	9.248	9.287	0.1	0.1	0.1	3.924	3.396	3.957	2.34	2.326	2.322	18.51	18.5	18.57	0.2	0.199	0.2	7.867	7.872	7.915	4.683	4.651	4.65	28.08	28.06	18.18	0.303	0.302	0.304	11.94	11.94	12.01	7.105	7.057	7.046
		9.031	9.026	9.071	0.1	0.099	0.099	4.361	4.364	4.384	2.61	2.597	2.593	18.06	18.05	18.14	0.198	0.198	0.196	8.723	8.728	8.767	5.221	5.192	5.186	27.4	27.39	17.52	0.301	0.3	0.301	13.23	13.24	13.3	7.921	7.877	7.868
		9.135	9.135	9.171	0.103	0.102	0.103	5.046	5.05	5.066	3.05	3.038	3.036	18.27	18.26	18.34	0.205	0.205	0.205	10.09	10.1	10.13	6.101	6.076	6.072	27.72	27.7	17.83	0.311	0.31	0.312	15.31	15.32	15.37	9.256	9.22	9.213
	positi on-3	9.312	9.313	9.315	0.1	0.1	0.101	3.927	3.923	3.948	2.329	2.337	2.311	18.62	18.63	18.63	0.201	0.201	0.201	7.855	7.846	7.897	4.658	4.674	4.622	28.26	28.26	18.16	0.305	0.304	0.305	11.92	11.9	11.98	7.067	7.092	7.013
		9.096	9.098	9.099	0.1	0.1	0.1	4.355	4.351	4.375	2.599	2.606	2.582	18.19	18.19	18.2	0.199	0.199	0.2	8.711	8.703	8.749	5.198	5.112	5.164	27.5	27.61	17.61	0.301	0.302	0.303	13.22	13.21	13.28	7.886	7.908	7.835
		9.196	9.198	9.2	0.103	0.103	0.103	5.041	5.037	5.058	3.04	3.046	3.025	18.39	18.4	18.4	0.206	0.206	0.206	10.08	10.08	10.11	6.08	6.092	6.051	27.9	27.91	17.92	0.313	0.312	0.313	15.3	15.29	15.35	9.226	9.243	9.181
	positi on-4	9.315	9.318	9.324	0.101	0.101	0.101	3.927	3.909	3.963	2.298	2.276	2.292	18.63	18.64	18.63	0.206	0.206	0.206	7.855	7.817	7.727	4.596	4.533	4.584	28.27	28.28	18.19	0.306	0.306	0.307	11.92	11.87	11.72	6.674	6.908	6.936
		9.098	9.103	9.107	0.1	0.1	0.1	4.352	4.335	4.29	2.588	2.547	2.561	18.2	18.21	18.2	0.2	0.2	0.201	8.705	8.669	8.582	5.137	5.094	5.122	27.61	27.62	17.64	0.304	0.304	0.305	13.21	13.15	13.02	7.794	7.729	7.772
		9.190	9.193	9.207	0.103	0.103	0.104	5.020	5.02	5.021	3.011	3.011	3.011	18.4	18.41	18.4	0.207	0.207	0.206	10.00	10.04	9.903	6.022	5.981	6.002	27.51	27.52	17.94	0.314	0.314	0.315	15.20	15.24	15.12	9.137	9.075	9.107

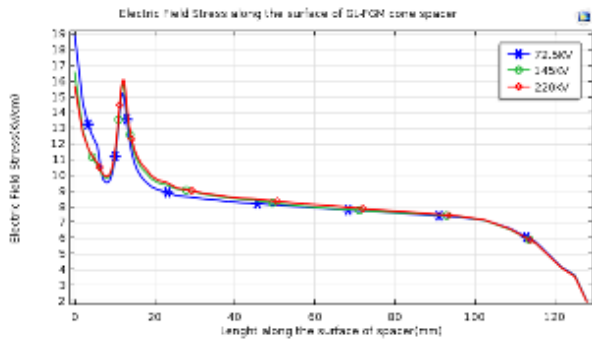
Table 1: At different applied voltages, Electric field stress in GH-FGM spacer for different dimensions and positions.



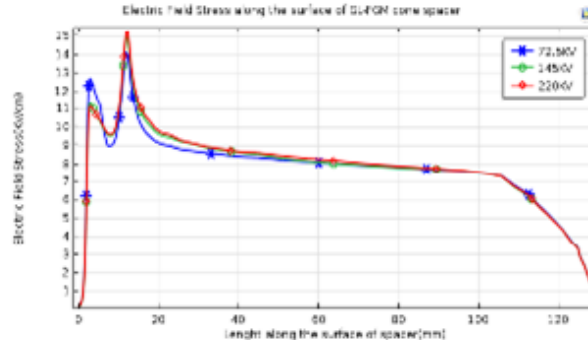
(a) At position 1 and dimension 1 without MI



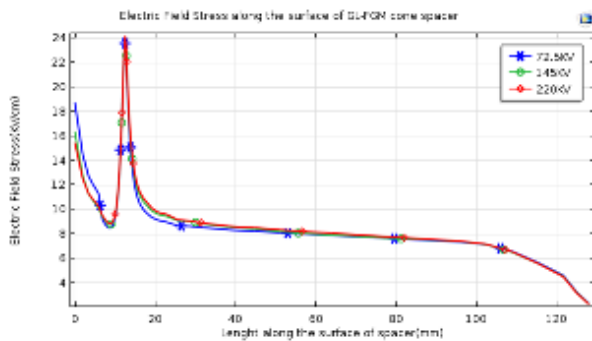
(b) At position 1 and dimension 2 with MI



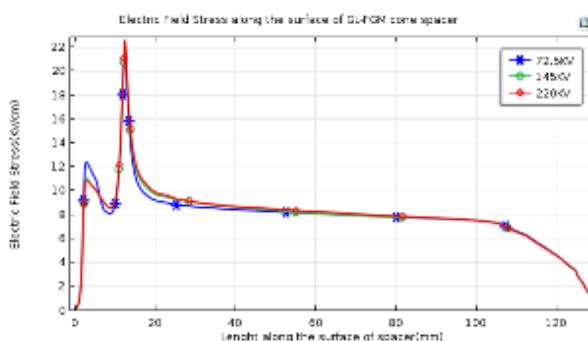
(c) At position 1 and dimension 2 without MI



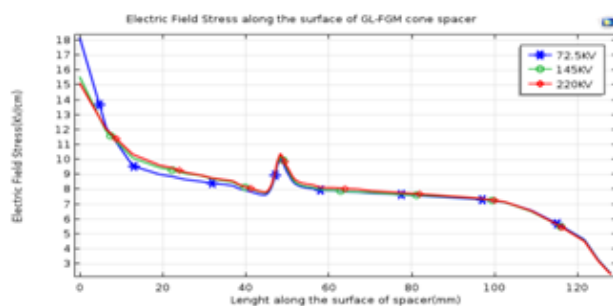
(d) At position 1 and dimension 2 with MI



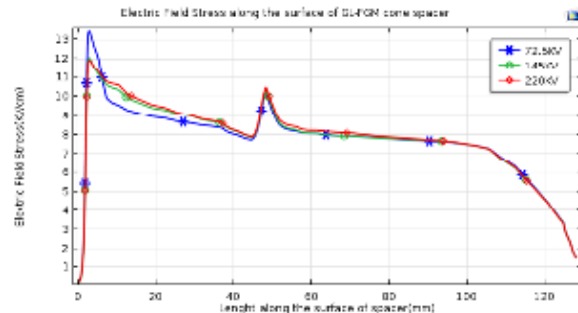
(e) At position 1 and dimension 3 without MI



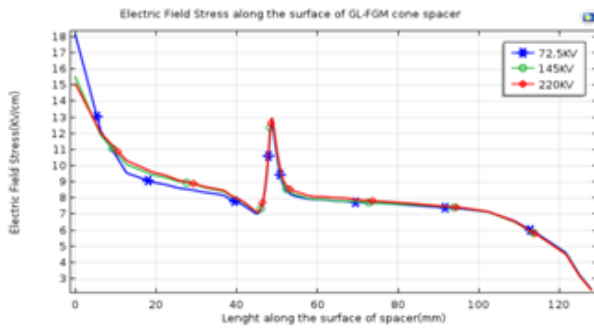
(f) At position 1 and dimension 3 with MI



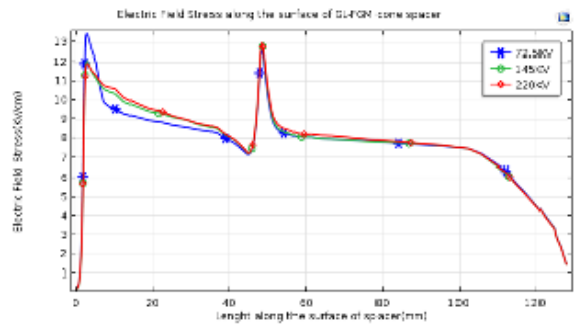
(g) At position 2 and dimension 1 without MI



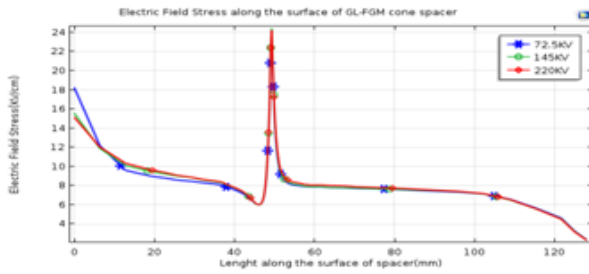
(h) At position 2 and dimension 1 with MI



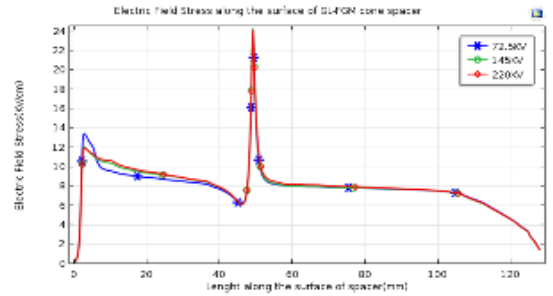
(i) At position 2 and dimension 2 without MI



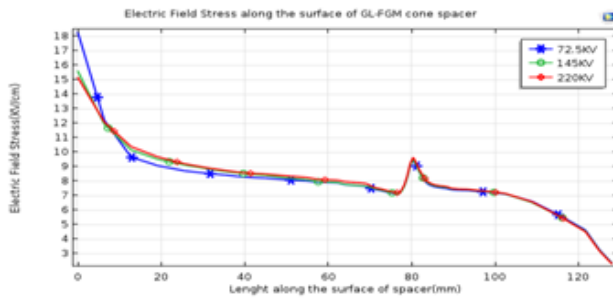
(j) At position 2 and dimension 2 with MI



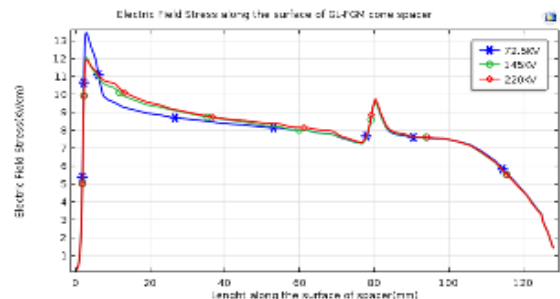
(k) At position 2 and dimension 3 without MI



(l) At position 2 and dimension 3 with MI



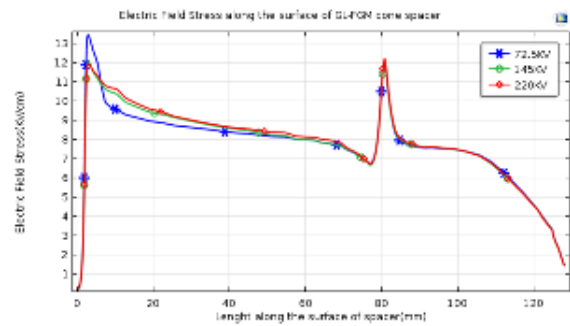
(m) At position 3 and dimension 1 without MI



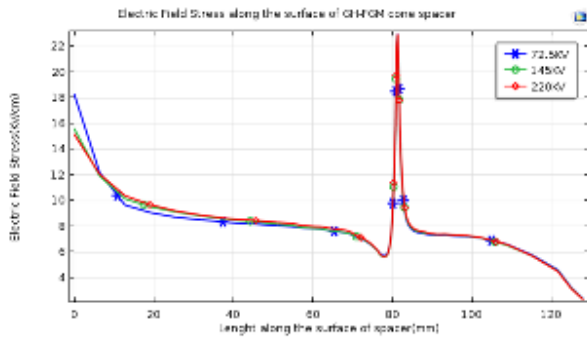
(n) At position 3 and dimension 1 with MI



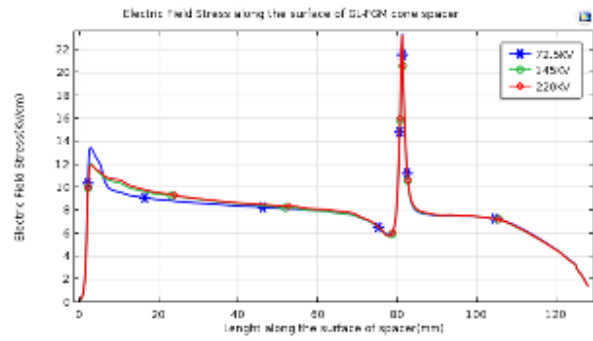
(o) At position 3 and dimension 2 without MI



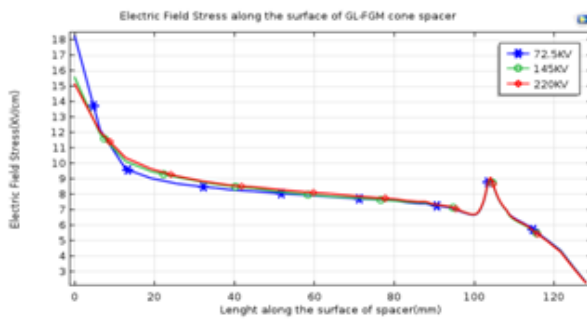
(p) At position 3 and dimension 2 with MI



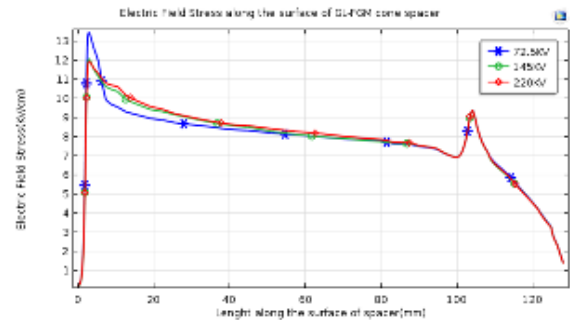
(q) At position 3 and dimension 3 without MI



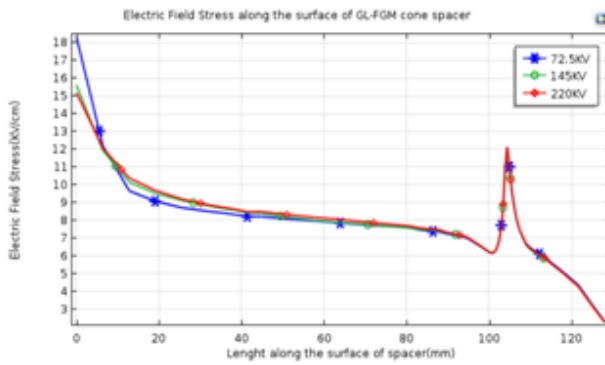
(r) At position 3 and dimension 3 with MI



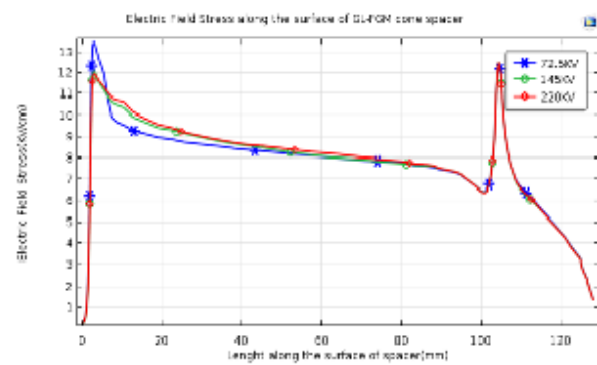
(s) At position 4 and dimension 1 without MI



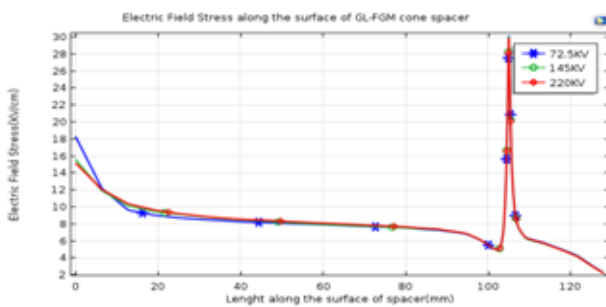
(t) At position 4 and dimension 1 with MI



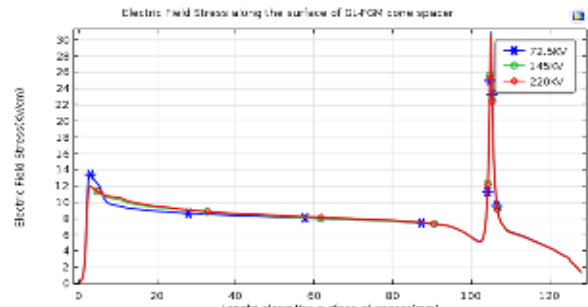
(u) At position 4 and dimension 2 without MI



(v) At position 4 and dimension 2 with MI



(w) At position 4 and dimension 3 without MI

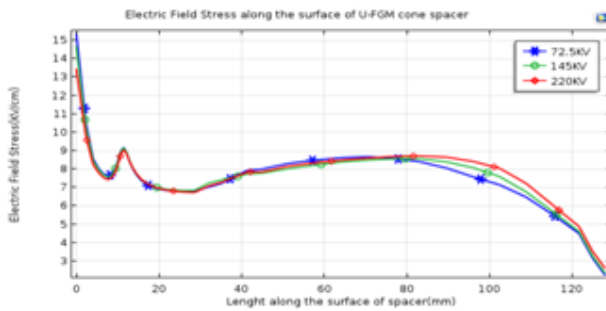


(x) At position 4 and dimension 3 with MI

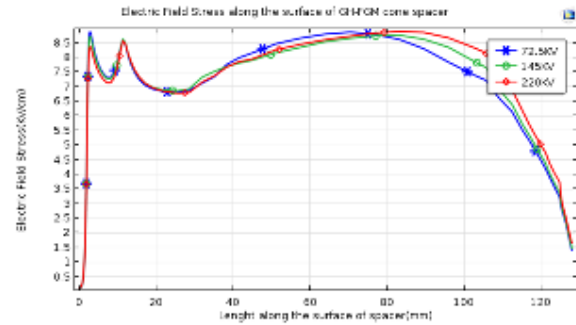
Fig. 3 Electric field stress for a GL FGM spacer for different dimensions and positions

Type	Applied Voltage	72.5kV									145kV									220kV																	
		Electric Field Stress Inner Electrode End (KV/CM)			Electric Field Stress outer Electrode End (KV/CM)			Electric Field Stress Inner Electrode End (KV/CM)			Electric Field Stress outer Electrode End (KV/CM)			Electric Field Stress Inner Electrode End (KV/CM)			Electric Field Stress outer Electrode End (KV/CM)																				
		vomi			vmi			vomi			vmi			vomi			vmi																				
		dim-1	dim-2	dim-3	dim-1	dim-2	dim-3	dim-1	dim-2	dim-3	dim-1	dim-2	dim-3	dim-1	dim-2	dim-3	dim-1	dim-2	dim-3																		
GH-FGM	position-1	19.2	19	18.75	0.231	0.228	0.226	2.324	1.973	2.326	1.428	1.431	0.451	38.39	38	37.49	0.462	0.458	0.451	+548	3.946	4.652	2.856	2.862	2.874	58.25	57.65	56.88	0.701	3.632	0.634	7.053	5.888	7.058	4.384	4.342	4.36
		16.18	16.61	16.38	0.206	0.204	0.201	2.296	1.95	2.298	1.434	1.42	0.401	33.6	33.22	32.76	0.412	0.401	0.401	+593	3.901	4.596	2.867	2.839	2.851	50.98	50.4	49.7	0.625	0.616	0.619	6.968	5.919	6.973	4.35	4.308	4.326
		15.94	15.72	15.46	0.208	0.204	0.202	2.274	1.933	2.276	1.445	1.414	0.403	31.87	31.43	30.92	0.415	0.401	0.403	+549	3.866	4.552	2.89	2.829	2.84	48.35	47.68	46.9	0.63	0.62	0.62	6.902	5.866	6.906	4.384	4.292	4.31
	position-2	18.2	18.2	18.2	0.241	0.24	0.241	2.324	2.326	2.346	1.445	1.429	1.426	38.41	38.39	38.54	0.482	0.48	0.482	+648	4.691	4.692	2.891	2.859	2.85	55.24	55.21	55.4	0.731	0.73	0.732	7.092	6.091	7.09	4.386	4.331	4.324
		15.56	15.56	15.58	0.216	0.216	0.216	2.296	2.298	2.318	1.434	1.418	1.414	31.12	31.11	31.17	0.432	0.43	0.433	+592	4.556	4.636	2.868	2.836	2.828	47.22	47.2	47.29	0.685	0.684	0.686	6.968	6.973	7.033	4.352	4.303	4.291
		15.14	15.13	15.5	0.219	0.218	0.219	2.274	2.276	2.296	1.429	1.413	1.409	30.27	30.26	30.3	0.437	0.431	0.438	+549	4.52	4.591	2.858	2.826	2.818	45.93	45.91	45.97	0.663	0.662	0.665	6.902	6.907	6.966	4.336	4.287	4.275
	position-3	18.31	18.32	18.32	0.242	0.242	0.242	2.316	2.312	2.336	1.432	1.411	1.411	36.33	36.64	36.65	0.483	0.481	0.481	+633	4.624	4.671	2.884	2.881	2.827	66.67	65.69	66.6	0.733	0.733	0.736	7.029	7.016	7.086	4.246	4.372	4.289
		16.62	16.62	16.62	0.217	0.217	0.217	2.289	2.289	2.307	1.421	1.429	1.403	31.23	31.24	31.24	0.434	0.431	0.434	+578	4.589	4.615	2.842	2.839	2.805	47.38	47.39	47.4	0.688	0.688	0.689	6.946	6.933	7.002	4.312	4.331	4.286
		15.18	15.18	15.9	0.219	0.219	0.22	2.267	2.263	2.285	1.416	1.424	1.397	30.36	30.36	30.37	0.439	0.431	0.44	+534	4.526	4.571	2.831	2.848	2.795	46.06	45.07	46.08	0.666	0.666	0.667	6.895	6.867	6.935	4.296	4.322	4.241
	position-4	18.32	18.32	18.33	0.243	0.243	0.243	2.31	2.293	2.251	1.404	1.385	1.402	36.33	36.65	36.67	0.485	0.481	0.486	4.62	4.566	4.503	2.809	2.769	2.803	55.58	55.6	55.63	0.736	0.736	0.738	7.01	6.958	6.832	4.261	4.203	4.253
		15.62	15.62	15.63	0.217	0.217	0.218	2.281	2.264	2.223	1.393	1.373	1.39	31.33	31.25	31.26	0.435	0.431	0.436	+563	4.529	4.447	2.786	2.747	2.781	47.39	47.41	47.43	0.66	0.66	0.662	6.924	6.872	6.748	4.228	4.168	4.22
		16.18	16.19	16.9	0.221	0.221	0.221	2.289	2.242	2.202	1.388	1.388	1.386	30.36	30.37	30.39	0.44	0.44	0.441	+579	4.485	4.404	2.776	2.737	2.772	46.07	45.08	46.1	0.688	0.688	0.69	6.896	6.809	6.883	4.212	4.163	4.205

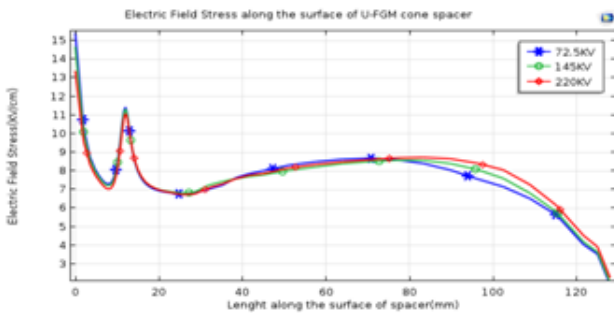
Table 2: At different applied voltages, Electric field stress in GL – FGM spacer for different dimensions and positions.



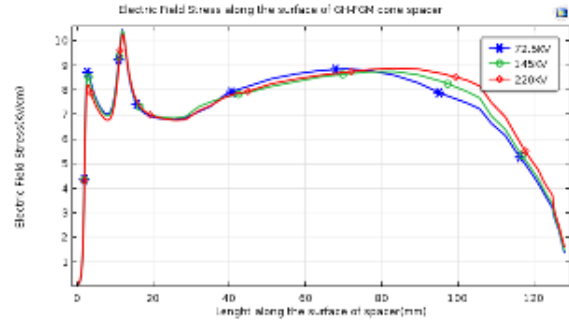
(a) At position 1 and dimension 1 without MI



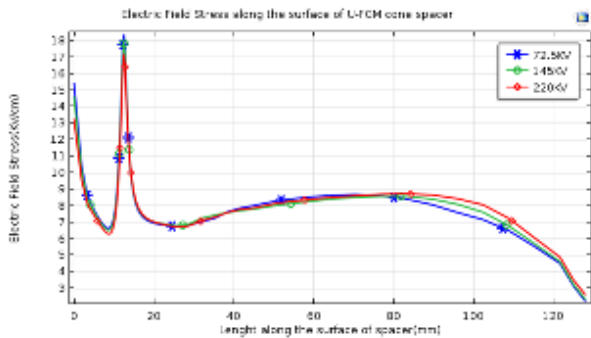
(b) At position 1 and dimension 1 with MI



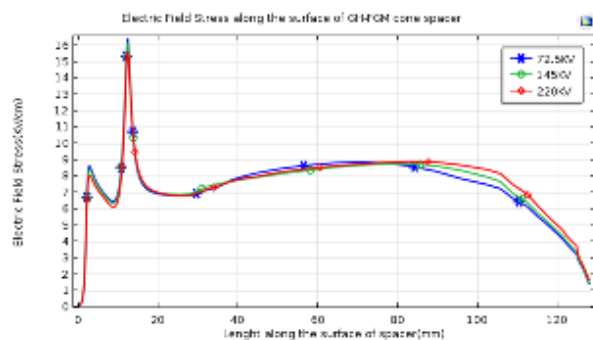
(c) At position 1 and dimension 2 without MI



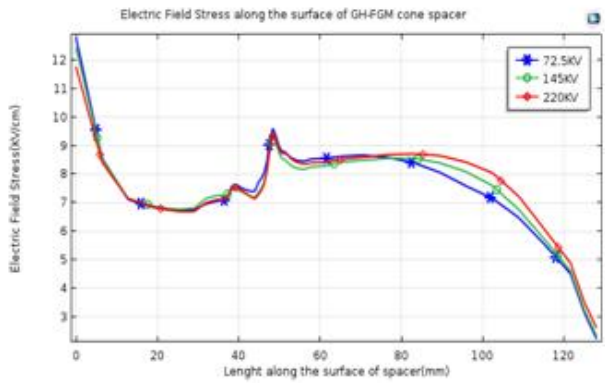
(d) At position 1 and dimension 2 with MI



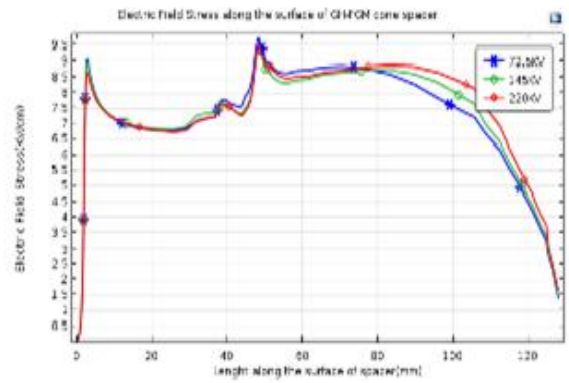
(e) At position 1 and dimension 3 without MI



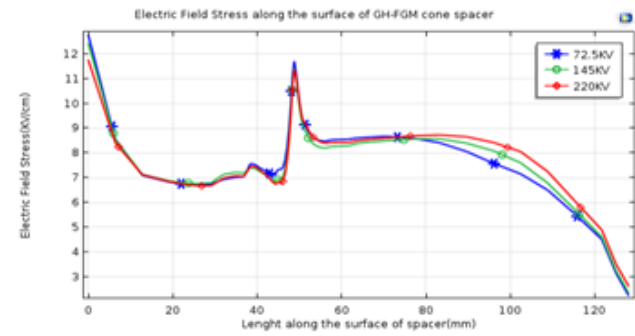
(f) At position 1 and dimension 3 with MI



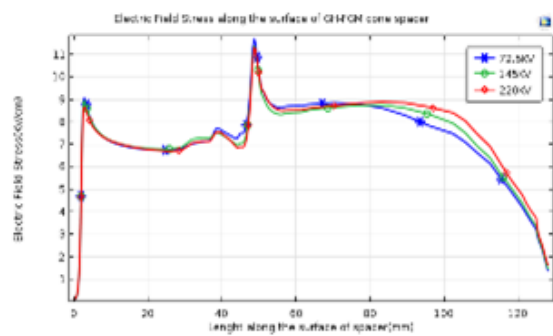
(g) At position 2 and dimension 1 without MI



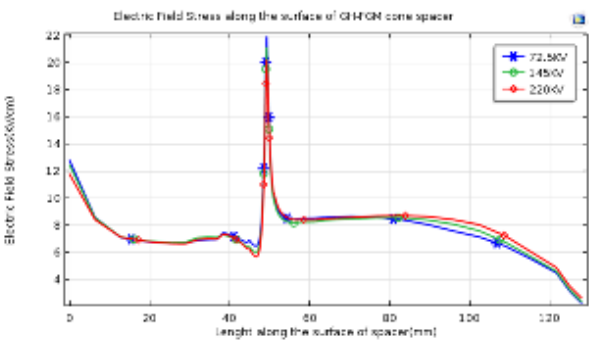
(h) At position 2 and dimension 1 with MI



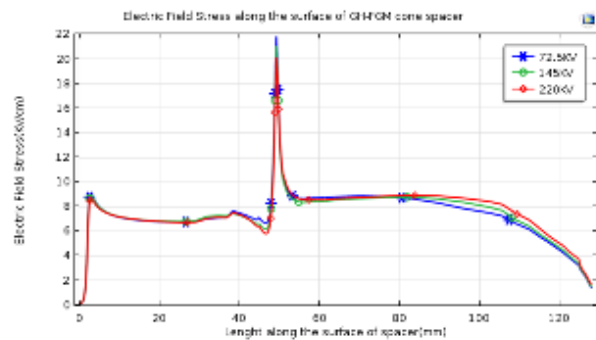
(i) At position 2 and dimension 2 without MI



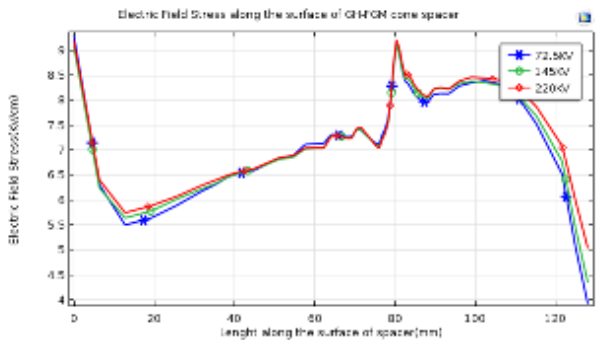
(j) At position 2 and dimension 2 with MI



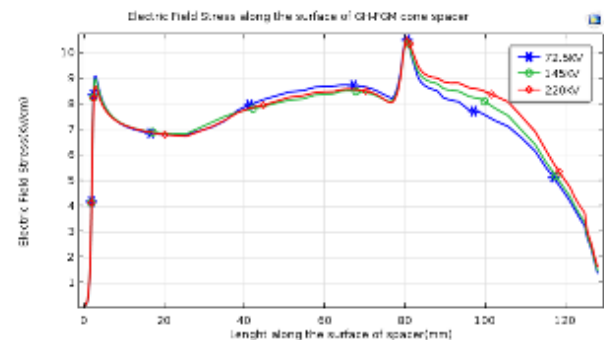
(k) At position 2 and dimension 3 without MI



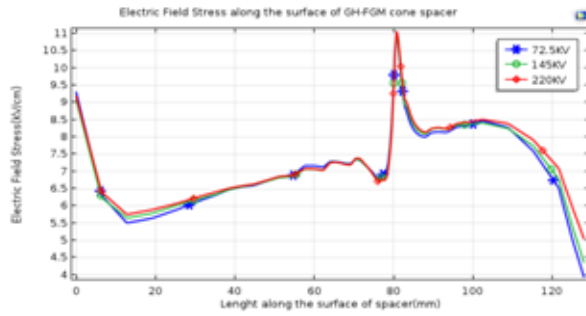
(l) At position 2 and dimension 3 with MI



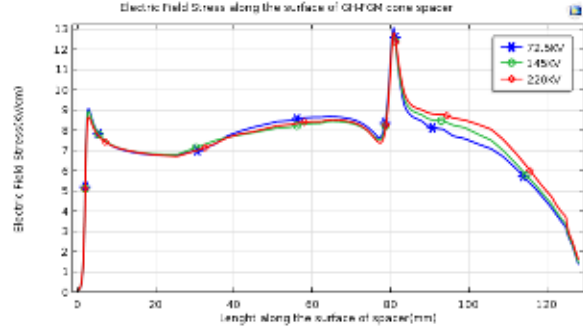
(m) At position 3 and dimension 1 without MI



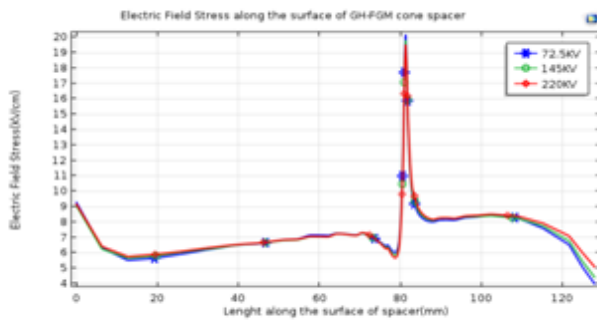
(n) At position 3 and dimension 1 with MI



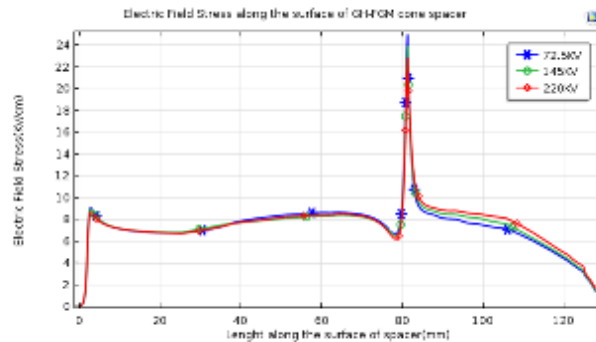
(o) At position 3 and dimension 2 without MI



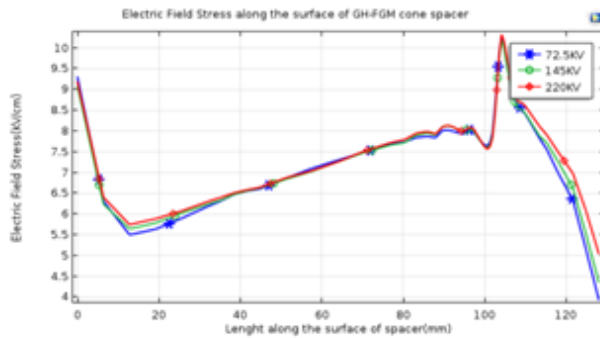
(p) At position 3 and dimension 2 with MI



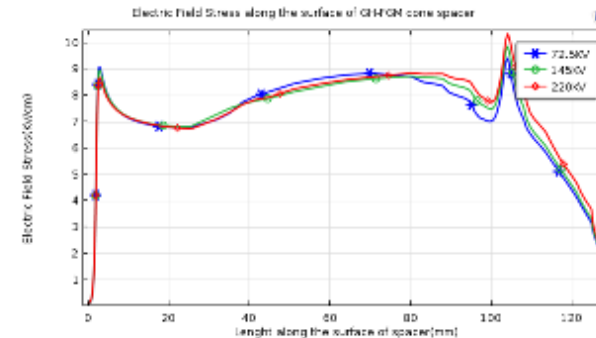
(q) At position 3 and dimension 3 without MI



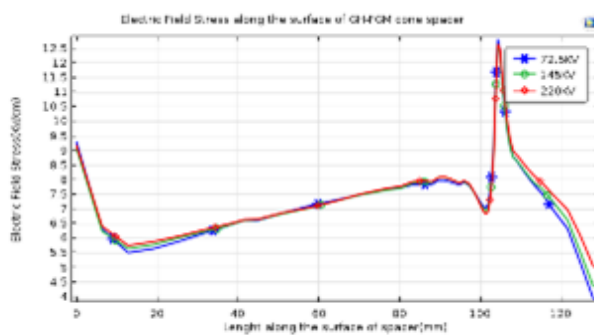
(r) At position 3 and dimension 3 with MI



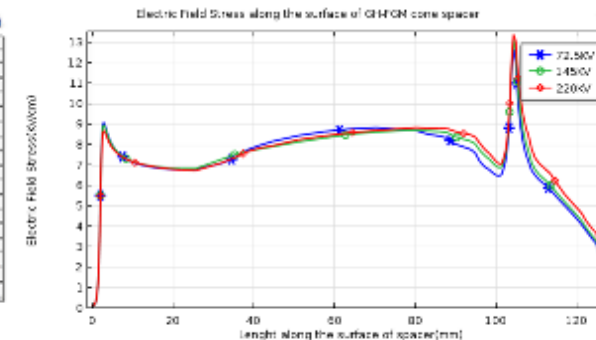
(s) At position 4 and dimension 1 without MI



(t) At position 4 and dimension 1 with MI



(u) At position 4 and dimension 2 without MI



(v) At position 4 and dimension 2 with MI

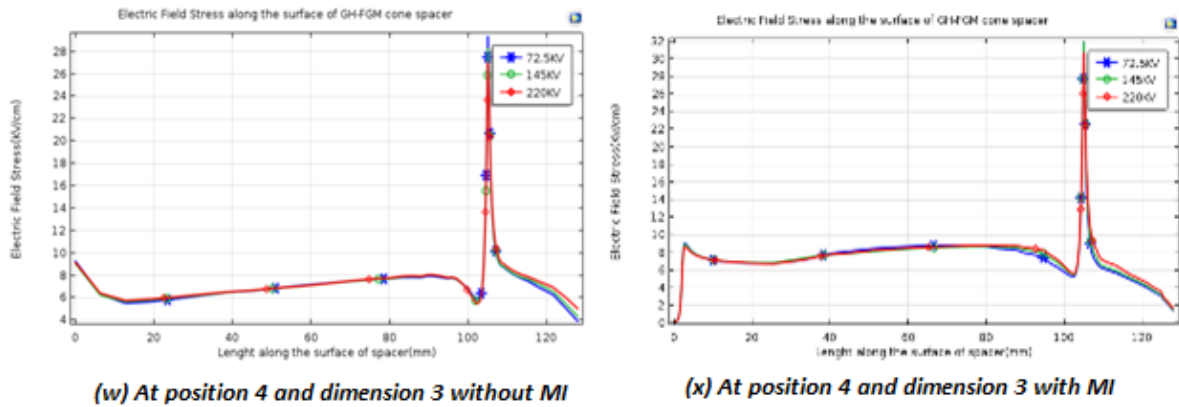


Fig. 4 Electric field stress for a U FGM spacer for different dimensions and positions

Applied Voltage	72.5kV												145kV												220kV											
	Electric Field Stress Inner Electrode End (kV/cm)						Electric Field Stress Outer Electrode End (kV/cm)						Electric Field Stress Inner Electrode End (kV/cm)						Electric Field Stress Outer Electrode End (kV/cm)						Electric Field Stress Inner Electrode End (kV/cm)						Electric Field Stress Outer Electrode End (kV/cm)					
	womi			wmi			womi			wmi			womi			wmi			womi			wmi			womi			wmi								
	dim 1	dim 2	dim 3	dim 1	dim 2	dim 3	dim 1	dim 2	dim 3	dim 1	dim 2	dim 3	dim 1	dim 2	dim 3	dim 1	dim 2	dim 3	dim 1	dim 2	dim 3	dim 1	dim 2	dim 3	dim 1	dim 2	dim 3	dim 1	dim 2	dim 3	dim 1	dim 2	dim 3			
positio n-1	15.39	15.43	15.46	0.141	0.14	0.14	2.222	1.869	1.222	1.386	1.372	1.377	30.78	30.86	30.91	0.261	0.279	0.279	4.443	3.737	4.444	1.772	2.743	2.754	46.71	46.82	46.9	0.426	0.424	0.423	6.741	5.67	6.741	4.205	4.162	4.179
	14.7	14.68	14.65	0.141	0.14	0.14	2.326	1.976	1.327	1.459	1.445	1.45	26.39	26.36	26.39	0.263	0.281	0.279	4.653	3.957	4.653	1.916	2.889	2.9	44.59	44.54	44.44	0.429	0.426	0.424	7.059	5.997	7.06	4.427	4.384	4.401
	11.46	11.38	11.27	0.141	0.14	0.138	2.6	2.255	1.601	1.631	1.617	1.623	26.93	26.75	26.54	0.267	0.279	0.277	5.2	4.51	5.201	2.261	3.234	3.245	40.84	40.59	40.27	0.429	0.424	0.42	7.89	6.844	7.891	4.948	4.906	4.923
positio n-2	12.8	12.79	12.84	0.144	0.144	0.145	3.934	3.936	3.957	1.387	1.37	1.366	25.6	25.59	25.69	0.289	0.288	0.289	4.444	3.787	4.444	2.774	2.741	2.732	38.84	38.82	38.97	0.438	0.437	0.439	6.743	6.747	6.808	4.209	4.159	4.145
	11.78	11.78	11.82	0.147	0.147	0.147	5.046	5.05	5.066	1.632	1.616	1.612	23.56	23.56	23.63	0.293	0.294	0.294	5.202	4.51	5.202	3.264	3.232	3.224	35.75	35.74	35.86	0.446	0.445	0.447	7.892	7.858	7.956	4.952	4.903	4.891
	11.87	11.88	11.88	0.145	0.145	0.145	2.215	2.21	2.215	1.374	1.362	1.355	25.75	25.76	25.75	0.29	0.29	0.291	4.43	3.781	4.43	2.747	2.734	2.709	39.07	39.08	39.09	0.44	0.44	0.441	6.721	6.708	6.778	4.168	4.194	4.11
positio n-3	11.59	11.59	11.54	0.147	0.147	0.147	2.52	2.518	2.096	1.447	1.436	1.428	25.06	25.06	25.07	0.295	0.295	0.294	4.64	4.654	4.654	3.284	2.911	2.857	28.02	28.05	28.04	0.445	0.445	0.446	7.04	7.028	7.099	4.251	4.217	4.264
	11.84	11.85	11.85	0.147	0.147	0.148	2.994	2.991	2.993	1.619	1.608	1.602	23.68	23.69	23.7	0.295	0.295	0.296	5.189	4.512	5.182	3.238	3.236	3.204	35.93	35.95	35.96	0.448	0.448	0.449	7.873	7.863	7.993	4.934	4.941	4.861
	11.88	11.88	11.88	0.146	0.145	0.146	2.208	2.19	2.148	1.345	1.325	1.342	25.75	25.78	25.77	0.291	0.291	0.292	4.416	3.81	4.416	2.651	2.685	3.007	39.08	39.08	39.1	0.442	0.441	0.443	6.7	6.648	6.513	4.038	4.023	4.073
positio n-4	11.53	11.53	11.54	0.147	0.147	0.148	2.312	2.294	2.252	1.418	1.399	1.415	25.06	25.07	25.08	0.294	0.295	0.294	4.585	4.505	4.505	2.796	2.83	3.002	38.04	38.05	38.05	0.447	0.447	0.448	7.016	6.962	6.835	4.303	4.242	4.293
	11.04	11.05	11.05	0.148	0.148	0.148	2.506	2.509	2.528	1.52	1.51	1.507	25.09	25.7	25.71	0.296	0.296	0.297	5.172	4.513	5.007	3.13	3.14	3.175	35.04	35.05	35.07	0.449	0.449	0.451	7.840	7.795	7.674	4.825	4.764	4.810

Table 3: At different applied voltages, Electric field stress in U – FGM spacer for different dimensions and positions.

REFERENCES

1. Nagesh Kumar et. al [42] showed that aluminum particle movement is more compared to copper in his study on random behavior of moving particles in both axial and radial directions using Monte Carlo method.
2. Nagesh Kumar, G.V., Amarnath, J., Singh, B.P., et al.: ‘Electric field effect on metallic particle contamination in a common enclosure gas insulated busduct’, IEEE Trans. Dielectr. Electr. Insul., 2007, 14, (2), pp. 334–340
3. Nagarjuna Reddy and Amarnath [54] in their research on metallic particle dynamics showed that with the increase of power frequency voltage, the peak movement also increases for any kind of metallic particle pollution.
4. Padmavathiet. al [14, 43] in their study on effect of impulse voltage like lightning in a 1-Ø GIB using gas mixtures proved that movement of particles is less in gas mixtures compared to pure SF6 gas. Also, movement of particle on epoxy coated insulator was obtained for various voltage levels.
5. H. Anis, K. D. Srivastava, “Free conducting particles in compressed gas insulation”, IEEE Transactions on Electrical Insulation, Vol. EI-16, pp. 327-338, 1981
6. F.Y. Chu “SF6 decomposition in gas insulated equipments”, IEEE transactions on electrical insulation volume.E-21 No. 5, October 1986
7. J. Amarnath, B.P. Singh, C. Radhakrishna and S. Kamakshaiha, Determination of Metallic particle trajectory in a Gas insulated Busduct predicted by Monte-Carlo technique, International Conference on Electrical Insulation and Dielectric Phenomena, October 17-21, 1999, Texas, Austin, USA.

BIOGRAPHY

G.V. Nagesh Kumar (M’06) was born in Visakhapatnam, India in 1977. He received the B.E. degree from College of Engineering, Gandhi Institute of Technology and Management, Visakhapatnam, India in 2000, the M.E. degree from the College of Engineering, Andhra University, Visakhapatnam, in 2003. He is presently pursuing his Doctoral degree from Jawaharlal Nehru Technological University, Hyderabad. He is also working as Associate Professor in the Department of Electrical and Electronics Engineering, Vignana’s Institute of Information Technology, Visakhapatnam. His research interests include gas insulated substations, fuzzy logic, high voltage testing and wavelets. He has published research papers in national and international conferences.